A comprehensive computational study of adatom diffusion on the aluminum (1 0 0) surface

J. Chapman[a], R. Batra[c], B.P. Uberuaga[b], G. Pilania[b], R. Ramprasad[a,*]

[a] Department of Materials Science & Engineering, Georgia Institute of Technology, Atlanta, GA, United States
[b] Materials Science & Technology Division, Los Alamos National Laboratory, Los Alamos, NM, United States
[c] Department of Materials Science & Engineering, University of Connecticut, Storrs, CT, United States

ABSTRACT

The complexity of adatom diffusion on the Al (1 0 0) surface is reflected by the existence of several low-energy non-trivial atomic exchange or vacancy formation mechanisms involving concerted motion of several (3–7) atoms. Interestingly, these mechanisms have energy barriers lower than or comparable to that of the simple (and intuitive) hopping mechanism commonly observed on other surface facets. While prior studies mainly used classical potentials to understand diffusion processes active on Al (1 0 0) surface, here we use accurate (and expensive) density functional theory (DFT) computations to estimate barriers associated with nine low-energy and non-trivial adatom diffusion mechanisms. We find that there exist several exchange mechanisms with energy barriers less than or equal to that of the trivial hop mechanism. Furthermore, several of the atomic exchange mechanisms have barriers within 0.2 eV of that of the simple hop, thereby highlighting mechanisms that can be relevant during surface/crystal growth. Our results paint a highly complex picture of the diffusion landscape on Al (1 0 0) and provide insights into how such mechanisms may contribute toward large length- and time-scale surface phenomena. The results presented in this work may also have implications for other fcc metals. Further, we show that some of the commonly used interatomic potentials fail to accurately capture the details of adatom diffusion on Al (1 0 0). The presented benchmark DFT dataset can thus be utilized to parameterize/retrain such potentials.

1. Introduction

Accurate surface dynamics of materials has become crucial due to its relevance in technologically relevant applications, such as catalysis, thin films, crystal growth and functional nano-materials. Although experiments based on field-ion microscopy (FIM) and scanning tunneling microscopy can be used to elucidate surface diffusion mechanisms and rates, the information available from these instruments is often limited in spatial and temporal resolution [1]. Computational methods based on density functional theory (DFT), on the other hand, allow us to estimate the energy barriers and reaction rates associated with plausible diffusion mechanisms. Typically, numerical approaches such as the nudged elastic band method (NEB) are used in conjunction with DFT to discover how energy pathways and transition state structures.

Self-diffusion of adatoms on the (1 0 0) surface of FCC metals is one particularly interesting problem [2,3]. For some metals, such as Al, Pt, Pd and Au, the adatom is known to diffuse by an exchange mechanism [4] (see Fig. 1a) where an adatom pushes a surface atom up onto the

surface, taking its place in the process. In contrast, for Cu and Rh, the adatom diffuses through a simple (and intuitive) hopping mechanism (see Fig. 1d) from one 4-fold site to next [5]. Furthermore, a multitude of non-trivial low-energy diffusion mechanisms have been shown to exist in the case of Al (1 0 0) surface [4,6–9]. The complexity of such mechanisms can be seen in Fig. 1. Besides exchange mechanisms being preferred over the hopping mechanism, past studies have also shown that some complex vacancy-based mechanisms (Fig. 1f, e) [6,7] have similar energy barriers to that of the intuitive hop. Such mechanisms have only been studied with classical parameterized potentials, however, and the question regarding which processes dominate the (1 0 0) crystal growth is yet to be answered.

The present study re-addresses and re-assesses the previously studied (using classical potentials) energy barriers of nine Al (1 0 0) surface diffusion mechanisms [6] using DFT, thus providing a robust benchmark for future similar studies. Nine mechanisms were chosen as they have been predicted to have relatively low energy barriers while capturing the diversity of the various processes, ranging from simple

exchange and hop to concerted multi-atom exchange and defect formations. We find that the 4-fold adatom hop does indeed have a potential energy barrier roughly three times that of the adatom-surface exchange, agreeing well with previous studies [10,11,4,8,9]. Further, our results suggest that there exist three exchange mechanisms with barriers lower than that of the 4-fold hop, as well as a number of highly complex exchange mechanisms with barriers within 0.2 eV of the 4-fold hop. We also find two vacancy formation mechanisms with similar barriers to the simple hop. Overall, these results paint an interesting picture where complex exchange/vacancy formation mechanisms dominate the surface diffusion on Al (1 0 0), which are expected to play a critical role during temperature aided processes such as crystal growth.

In addition to providing a benchmark set of results pertaining to complex adatom diffusion mechanisms on the Al (1 0 0) surface, this work also reveals some of the deficiencies of known classical interatomic potentials. In particular, we show that some of the routinely used embedded atom method (EAM) based potentials do not consistently reproduce the DFT energy barriers for some mechanisms. While some barriers are correctly captured, others are overestimated, which may impact the results of dynamical simulations. The DFT data generated in

this work can be used to develop/train better potentials (both classical or machine learning based [12–14]) that accurately capture this complex surface science phenomenon.

The outline of this paper is as follows. First, a detailed description of the nine mechanisms studied in this work is provided. The computational details are discussed next. The primary results are then presented, showcasing the various minimum energy pathways predicted by DFT and the Voter [15], Liu [16] and Mishin [17] EAM potentials. We then conclude by discussing the implications of this work, and highlighting a pathway for how this data can be used for a variety of other large-scale computational methods.

2. Theoretical methods

2.1. Al (1 0 0) surface diffusion mechanisms

We have created a catalog of nine mechanisms, varying in both energy and physical complexity, guided by previous work [6,7,18]. These nine mechanisms involve atomic exchange, hopping, and vacancy-formation, all involving the same initial configuration of a single adatom on an otherwise clean (1 0 0) surface. All nine mechanisms are
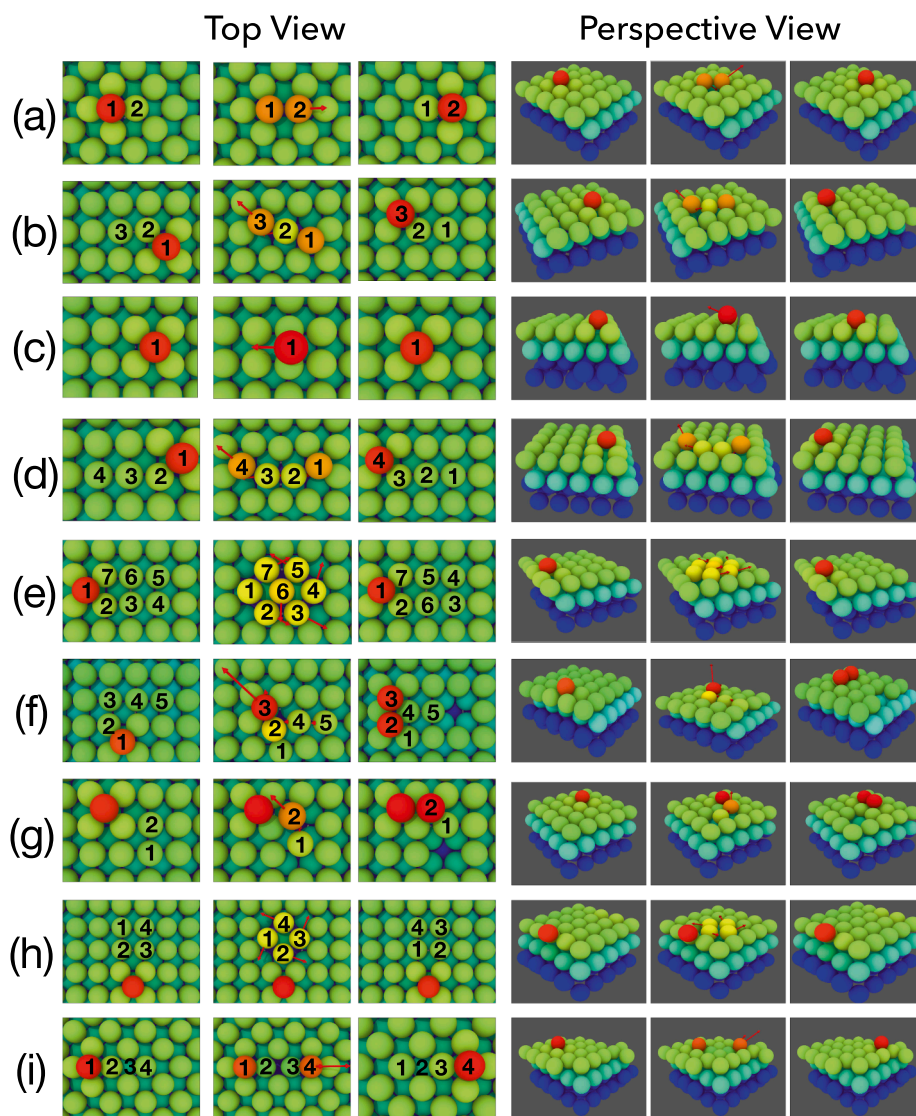

Fig. 1. The top and perspective views of the nine surface diffusion mechanisms studied in this work. Moving from left to right, the initial, mid-point, and final configurations along the reaction pathway are presented in each view. The atoms are colored corresponding to their height along the surface normal to serve as a guide to the eye. For each mechanism, relevant atoms are numbered to help track their trajectory, and red arrows are used to indicate current trajectory of the atoms. (For interpretation of the references to colour in this figure legend, the reader is referred to the web version of this article.)

described in detail throughout this section. The mechanisms are labeled **a–i** in the order of increasing barrier height; **a** corresponds to the lowest and **i** to the mechanism with highest barrier energy. In the case where multiple barriers exist along a given pathway, the largest among them is reported as the barrier corresponding to that mechanism. All nine mechanisms are illustrated in Fig. 1.

Mechanism **a** corresponds to the previously discussed two-atom exchange involving an adatom and a surface atom. The adatom pushes a surface atom up onto the surface, taking its place in the process. Mechanism **b** is a 3-atom exchange where an adatom pushes its way into the surface, causing 2 surface atoms to move within the surface plane until the furthest surface atom involved in the exchange is pushed up onto the surface as an adatom. The most simple and intuitive mechanism considered in this work is Mechanism **c** which involves an adatom hopping from one 4-fold site to another, as stated earlier. Mechanism **d** is a 4-atom exchange where an adatom pushes its way into the surface, causing 3 surface atoms to move in a line, within the surface plane, until the furthest surface atom is pushed onto the surface as a new adatom.

Mechanism **e** is a highly complex set of atomic exchanges where various atoms swap positions. This mechanism, as dilettante as it may sound, is reminiscent of a game of musical chairs. The adatom first exchanges with a surface atom, which in turn exchanges, within the surface plane, with a neighboring atom. This process of surface-plane exchange continues in a circular path until the original adatom is pushed back atop the surface to its original position. While the adatoms initial and final positions remain constant, the various surface atoms involved have all exchanged places. This mechanism is arguably the most structurally complex of the nine mechanisms considered here, as reflected by the presence of multiple saddle points along the potential energy surface (PES), to be discussed later (see Fig. 2).

Mechanism **f** is a 2-part exchange and vacancy creation involving 5 atoms. The first process involves an adatom exchanging with its nearest surface atom, which in turn exchanges with a neighboring surface atom, pushing that atom onto the surface. This process is identical to mechanism **b**. The second part of this process involves 3 surface atoms exchanging, one of which gets pushed onto the surface. This ultimately creates 2 adjacent adatoms, and a surface vacancy.

Mechanism **g** is a vacancy formation mechanism involving a surface atom pushing upon an adjacent surface atom on top of the surface. This new adatom sits adjacent to another adatom. Mechanism **h** involves 4 surface atoms rotating parallel to the surface plane, similar to that of a spinning windmill. At the center of the axis of rotation for the 4 surface atoms exists a 4-fold site. An adatom is located two 4-fold sites away, following any arbitrary straight path. The adatom is not directly involved in the mechanism, but does exert its influence by keeping all exchanging atoms to the surface plane.

Mechanism **i** involves two surface layers rather than one. An atom on the second layer pushes an atom above it until that atom eventually makes its way above the surface as an adatom, where the second layer atom now takes its place. Having a vacancy now formed in the second layer, another adatom pushes down on a surface atom, which in turn rushes to fill the vacancy, with the second adatom taking its place. Images and movies were rendered using the Ovito software package [19]. All data pertaining to this work are available at our data repository, Khazana (https://khazana.gatech.edu).

2.2. Computational details

The energy barriers for the aforementioned surface diffusion mechanisms were studied using DFT and EAM to allow for a systematic and consistent comparison. The DFT calculations were performed on a 4-layer slab containing 101 atoms, plus any adatoms. The bottom layer remained fixed, giving the impression of a bulk-like region. All DFT calculations were done using the Vienna Ab Initio Simulation Package (VASP) [20,21]. The Perdew-Burke-Ernzerhof (PBE) functional [22] was used to calculate the electronic exchange-correlation interaction. Projector augmented wave (PAW) potentials and plane-wave basis functions up to a kinetic energy cutoff of 500 eV were used [23]. All projection operators (involved in the calculation of the non-local part of the PAW pseudopotentials) were evaluated in the reciprocal space to ensure further precision. The NEB routine [24,25], along with the climbing image method [26] in the Transition State Tools package, was used with DFT energy calculations to predict the lowest energy pathway for each mechanism. Ionic relaxations were considered converged at an energy difference of 10^{-2} eV, and the electronic convergence was terminated at an energy difference of 10^{-5} eV.

EAM calculations were performed using a 5-layer slab of Al (1 0 0) containing 126 atoms, plus any adatoms. The bottom 2 layers remained fixed, making this structurally identical to the DFT slab. As mentioned earlier, three EAM potentials were considered (created by Voter, Liu, and Mishin) [15–17], henceforth referred to as EAM-V, EAM-L, EAM-M. EAM-V was chosen as it was used previously to predict the barrier heights of all mechanisms considered in this work [6,7]. EAM-M was chosen due to its popularity and ability to reproduce several mechanical and thermal properties of Al [17,27,28], but lack of study with regards to the surface behavior. Similarly, EAM-L was chosen owing to its success in reproducing complex behavior in good agreement with DFT [16].

All EAM calculations were performed using the Large-scale Atomic/Molecular Massively Parallel Simulator (LAMMPS) [29]. Potential energy barriers were calculated using the NEB routine in tandem with the climbing image formalism. Owing to relatively low computational cost, a stricter convergence criteria of 10^{-5} eV/Å for forces and 10^{-8} eV for energy were used.

For all levels of theory, barrier heights were calculated with respect to the global barrier height, regardless of the number of local minima along a given reaction pathway. Such a definition stems from the assumption that the intermediate states can be assumed to be at steady state. From this assumption it can be shown that the largest barrier will dominate the overall reaction rate [30,31].

3. Results and discussion

3.1. DFT results

Fig. 2 showcases the minimum energy profiles for all nine mechanisms considered, while Table 1 and Fig. 3 summarize the potential energy barrier heights. Some available literature results, also calculated using DFT but with different exchange–correlation functionals, are included and show good agreement with our computed values. We see that the adatom-surface exchange, mechanism **a**, has a potential energy barrier roughly 3 times less than that of the 4-fold adatom hop, mechanism **c**. As stated previously, mechanisms **b** and **d** also have a potential barrier less than or equal to that of the 4-fold adatom hop. Mechanisms **e** and **f** show a barrier within 0.2 eV of the hop, indicating they could occur with similar frequency. Mechanisms **g** through **i** yield substantially larger barriers and thus are predicted to occur less frequently.
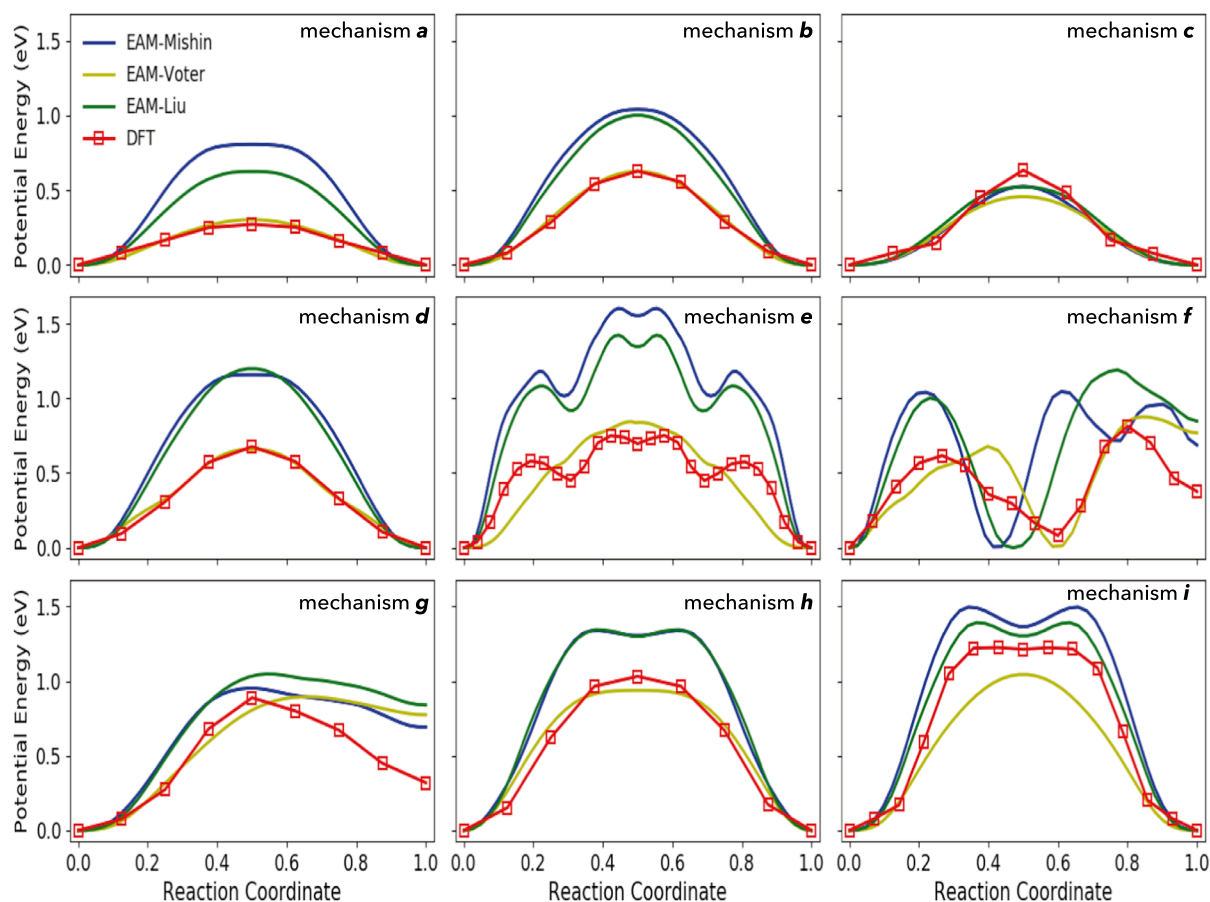
Fig. 2. Minimum energy profiles for all nine mechanisms studied in this work using DFT, and EAM-V,C, and M. Mechanisms are organized in the order of increasing DFT potential energy barriers.

Table 1

Al (1 0 0) surface diffusion energy barriers, as computed using DFT, and EAM-V, EAM-L, and EAM-M, for the nine mechanisms considered in this work. Past computations are included in brackets.

Mechanism	Type	DFT (eV)	EAM-V (eV)	EAM-L (eV)	EAM-M (eV)
a	Exchange	0.27	0.30	0.63	0.81
		(0.20 [4])	(0.23 [6])		
b	Exchange	0.63	0.63	1.00	1.04
			(0.43 [6])		
c	hop	0.63	0.46	0.52	0.53
		(0.65 [4])	(0.372 [6])		(0.48 [32])
d	Exchange	0.68	0.66	1.20	1.16
		(0.50 [18])	(0.41 [6])		
e	Exchange	0.75	0.84	1.42	1.60
			(0.60 [6])		
f	Vacancy	0.81	0.88	1.19	1.05
			(0.75 [6])		
g	Vacancy	0.89	0.90	1.05	0.95
			(0.77 [6])		
h	Exchange	1.03	0.94	1.33	1.34
			(0.70 [6])		
i	Exchange	1.22	1.04	1.38	1.49
			(0.91 [6])		

3.2. EAM results

We again direct the reader's attention to Table 1 and Figs. 2 and 3 for a detailed portrayal of transition state energies for the three EAM potentials considered. It is evident from the results that the EAM calculations show some level of deviation from DFT. EAM-V outperforms the other two potentials. Although, it fails to accurately predict the topology of the energy landscape when multiple local minima exist (e.g. mechanisms **e** and **f**), the global barrier of such mechanisms is still captured well. The most significant deviation from DFT is its underprediction of the 4-fold hop's barrier, causing it to be the second lowest barrier.

From Table 1 it can be observed that the overall trend in the computed barriers of EAM-V in this work are over-estimated compared to those reported from previous work. These differences can be attributed to the surface unit cell area of the structures considered here. Previous work has shown that the surface unit cell can have a significant impact on the calculated potential energy barriers [5]. However, due to computational limitations when using DFT, smaller surface unit cells, when compared to previous work, are considered for all levels of theory to ensure consistency. Another source of error can be attributed to how the potential was implemented by different researchers; for example, how the cutoffs were treated. Overall, the trend in barrier height is the same for all EAM potentials, regardless of surface unit cell chosen, and therefore the conclusions drawn regarding how such processes affect the long time-scale behavior should remain consistent.

Fig. 2 clearly suggests that both EAM-L and EAM-M over-estimate the energy barrier for almost all mechanisms. Naturally, due to this inconsistency in barrier heights, the rate of occurrence of each of these mechanism will be substantially lower than that predicted by DFT during molecular dynamics simulations. Further, elevated temperatures will be needed to activate these mechanisms. Interestingly, EAM-L and EAM-M perform more adequately in terms of the nature of the PES for the various mechanisms when compared to EAM-V (see Fig. 2b); for cases with multiple DFT transition states, EAM-V predicts a single transition state. Thus, no single EAM potential can completely describe the complex nature of adatom surface diffusion on Al (1 0 0). Although
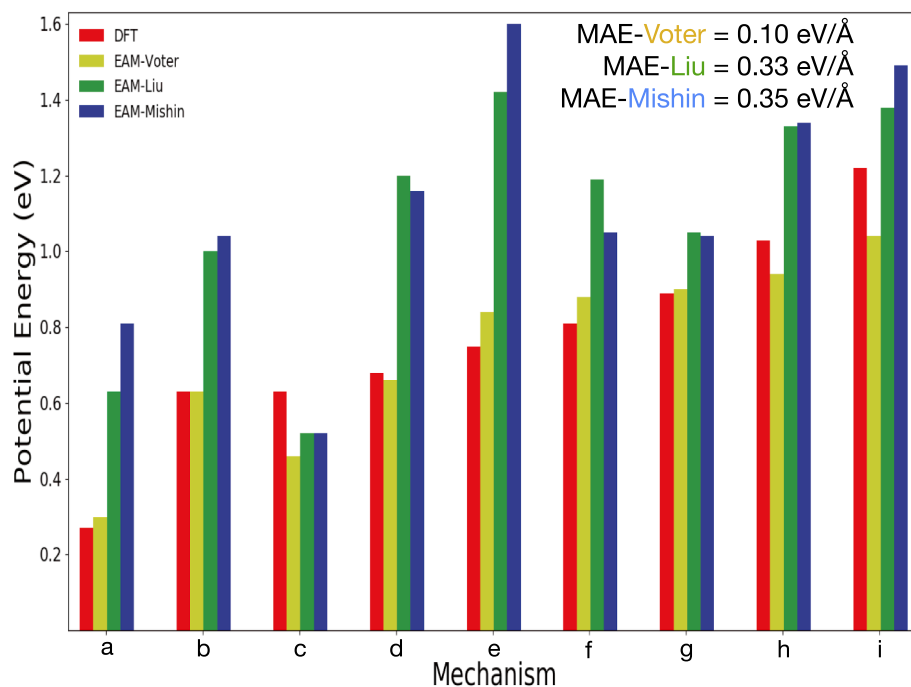
Fig. 3. Transition state energies of all mechanisms compared for all levels of theory. The mean absolute error (MAE) between all EAM potential and DFT for all potential energy barriers is also reported in the top of the figure.

further studies are required to establish the cause of discrepancy between DFT and EAM potentials, a simple explanation could be the incapability of the EAM functional form to account for the complex nature of bonding present in these different surface phenomena.

3.3. Discussion

We first restrict the focus of our discussion to the implications of the DFT results. The combination of complexity and low-energy barriers seen here for exchange and vacancy-based mechanisms dwarfs that of the hop-based mechanism. There can conceivably be a plethora of other non-hopping mechanisms with potential barriers comparable to that of the hopping mechanism **c**. Due to the fact that hopping is inhibited by its large potential barrier, exchange mechanisms would appear to dominate Al (1 0 0) surface diffusion. Vacancy creation and hopping mechanisms appear to have similar barriers, and thus could occur with similar probability during high temperature molecular dynamics simulations.

This scenario could lead to vacancy-based mechanisms aiding crystal growth under the appropriate conditions. Vacancy mechanisms generate new adatoms by forcing surface atoms up onto the surface. In dynamic environments some fraction of a given monolayer will be composed of such atoms. Therefore, vacancy-based mechanisms could influence properties such as the nucleation of islands. These mechanisms could also influence the rate of adsorbants onto the surface, as the creation of new adatoms can lead to the depletion of active sites.

EAM potentials, with the exemption of the EAM-V potential, generally tend to over-estimate the energy barrier relative to DFT. Barrier heights for all mechanisms and levels of theory are compared in Fig. 3, highlighting the differences between DFT and EAM. These discrepancies establish the need for more accurate interatomic potentials that accurately capture the complexity of surface phenomena on Al (1 0 0). Going forward, the data—surface diffusion barriers and pathways—emerging from the present contribution can be used to create better surface science oriented interatomic potentials (semi-empirical, machine learning [12–14], etc.) that can be used to study large length-scale and time-scale dynamics, such as nucleation and crystal growth.

4. Conclusion

In summary, we have explored a variety of surface diffusion mechanisms of an adatom on the Al (1 0 0) surface using DFT, and three different EAM potentials. Inspired from past studies, we considered nine mechanisms that differ significantly in terms of their structural and energetic complexity. Our DFT results suggest that multiple atomic exchange mechanisms (involving concerted motion of 3–7 atoms) have lower energy barrier than the simple (and intuitive) adatom hopping mechanism, making the diffusion phenomena on (1 0 0) surface particularly unique. Further, we find several vacancy formation mechanisms to have energy barriers comparable to that of the hopping mechanism. Thus, at moderate temperatures, we predict vacancy formation mechanisms to serve as an energetically "inexpensive" way of adding adatoms to free surface layers, which will play a crucial role in island nucleation and crystal growth.

As modeling of large length- and time-scale phenomena such as crystal growth are beyond the present capabilities of DFT, inexpensive potentials that accurately capture diverse surface processes must be used. However, as shown in this work, commonly used classical potentials may have difficulties in accurately capturing the diffusion mechanisms on the Al (1 0 0) surface, and thus, are consequently the corresponding surface dynamics. Nonetheless, the DFT data generated in this work could be used to parameterize such interatomic potentials or force fields to correctly account for relevant diffusion mechanisms.

5. Data Availability

The raw data required to reproduce these findings are available to download from https://khazana.gatech.edu. The processed data required to reproduce these findings are available to download from https://khazana.gatech.edu.

Acknowledgments

Appendix A. Supplementary material

Supplementary data associated with this article can be found, in the online version, at https://doi.org/10.1016/j.commatsci.2018.11.032.

References

[1] M.C. Tringides, Surface Diffusion: Atomistic and Collective Processes, Springer, Boston, MA, 1997.

[2] G. Kellogg, Field ion microscope studies of single-atom surface diffusion and cluster nucleation on metal surfaces, Surf. Sci. Rep. 21 (1) (1994) 1–88, https://doi.org/10.1016/0167-5729(94)90007-8 URL http://www.sciencedirect.com/science/article/pii/0167572994900078.

[3] B.D. Yu, M. Scheffler, Physical origin of exchange diffusion on fcc(1 0 0) metal surfaces, Phys. Rev. B 56 (1997) R15569–R15572, https://doi.org/10.1103/PhysRevB.56.R15569.

[4] P. Feibelman, Diffusion path for an al adatom on Al(001), Phys. Rev. Lett. 65 (1990) 729–732.

[5] C.M. Chang, C.M. Wei, Self-diffusion of adatoms and dimers on fcc (1 0 0) surfaces, Chin. J. Phys. 43 (1S) (2005) 169–175.

[6] G. Henkelman, H. Jònsson, A dimer method for finding saddle points on high dimensional potential surfaces using only first derivatives, J. Chem. Phys. 111 (1999) 7010–7022.

[7] G. Henkelman, H. Jònsson, Long time scale kinetic Monte Carlo simulations without lattice approximation and predefined event table, J. Chem. Phys. 115 (2001) 9657–9666.

[8] P. Gravil, S. Holloway, Exchange mechanisms for self-diffusion on aluminum surfaces, Surf. Sci. 310 (1993) 267–272.

[9] R. Stumpf, M. Scheffler, Ab initio calculations of energies and self-diffusion on flat and stepped surfaces of al and their implications on crystal growth, Phys. Rev. B 53 (1996) 4958–4973.

[10] F. Montalenti, Transition-path spectra at metal surfaces, Surf. Sci. 543 (2003) 141–152.

[11] S. Yunsic, V. Borovikov, B. Uberuaga, A. Voter, J. Amar, Vacancy formation and strain in low-temperature Cu/Cu (1 0 0) growth, Phys. Rev. Lett. 101 (2008).

[12] V. Botu, R. Batra, J. Chapman, R. Ramprasad, Machine learning force fields: construction, validation, and outlook, J. Phys. Chem. C 121 (2016) 511–522, https://doi.org/10.1021/acs.jpcc.6b10908.

[13] V. Botu, R. Ramprasad, Learning scheme to predict atomic forces and accelerate materials simulations, Phys. Rev. B 92 (2015).

[14] H. Tran, V. Botu, R. Batra, Chapman, S. Krishnan, L. Chen, R. Ramprasad, A universal strategy for the creation of machine learning-based atomistic force fields, npj Comp. Mat. 3 (2017) 1–8, https://doi.org/10.1038/s41524-017-0042-y.

[15] A. Voter, S. Chen, Accurate interatomic potentials for Ni, Al, and Ni3Al, Mater. Res. Soc. 82 (1987) 175.

[16] X. Liu, F. Ercolessi, J. Adams, Aluminium interatomic potential from density functional theory calculations with improved stacking fault energy, Modell. Simul. Mater. Sci. Eng 82 (2004) 175, https://doi.org/10.1088/0965-0393/12/4/007.

[17] R. Zope, Y. Mishin, Interatomic potentials for the Ti-Al system, Phys. Rev. B, 68. https://doi.org/10.1103/PhysRevB.68.024102.

[18] G. Henkelman, H. Jònsson, Multiple time scale simulations of metal crystal growth reveal the importance of multiatom surface processes, Phys. Rev. Lett. 90 (2003) 259–263, https://doi.org/10.1103/PhysRevLett.90.116101.

[19] A. Stukowski, Visualization and analysis of atomistic simulation data with ovito—the open visualization tool, Modell. Simul. Mater. Sci. Eng 18 (1) (2010) 015012 URL http://stacks.iop.org/0965-0393/18/i=1/a=015012.

[20] G. Kresse, J. Furthmüller, Efficient iterative schemes for ab initio total energy calculations using a plane-wave basis set, Phys. Rev. B 54 (1996).

[21] G. Kresse, D. Joubert, From ultrasoft pseudopotentials to the projector augmented wave method, Phys. Rev. B 59 (1999).

[22] J.P. Perdew, K. Burke, Y. Wang, Generalized gradient approximation for the exchange-correlation hole of a many electron system, Phys. Rev. B 54 (1996).

[23] P.E. Blöchl, Projector augmented wave method, Phys. Rev. B 50 (1994).

[24] H. Jònsson, G. Mills, K.W. Jacobsen, Nudged elastic band method for finding minimum energy paths of transitions, Class. Quant. Dynam. Condens. Phase Simul. 50 (1998) 385.

[25] H. Jònsson, G. Henkelman, Improved tangent estimate in the nudged elastic band method for finding minimum energy paths and saddle points, J. Chem. Phys 113 (2000).

[26] H. Jònsson, G. Henkelman, B. Uberuaga, A climbing image nudged elastic band method for finding saddle points and minimum energy paths, J. Chem. Phys. 113 (2000).

[27] J. Wang, A. Horsfield, P. Lee, P. Brommer, Heterogeneous nucleation of solid al from the melt by al3ti: molecular dynamics simulations, Phys. Rev. B 82 (2010).

[28] E. Levchenko, A. Evteev, G. Löwisch, I. Belova, G. Murch, Molecular dynamics simulation of alloying in a ti-coated al nanoparticle, Intermetallics 22 (2011) 192–203.

[29] S. Plimpton, Fast parallel algorithms for short-range molecular dynamics, J. Comput. Phys. 117 (1) (1995) 1–19, https://doi.org/10.1006/jcph.1995.1039 URL http://lammps.sandia.gov/.

[30] D. Wales, Energy landscapes: calculating pathways and rates, Int. Rev. Phys. Chem. 25 (2006) 237–282.

[31] J. Murdoch, What is the rate-limiting step of a multistep reaction? J. Chem. Educat. 58 (1981) 32–36.

[32] H. Hanchen, J. Wang, Surface kinetics: step-facet barriers, Appl. Phys. Lett. 83 (2003) 4752–4754.